

A microfluidic photobioreactor array demonstrating high-throughput screening for microalgal oil production†

 Cite this: *Lab Chip*, 2014, 14, 1415

 Hyun Soo Kim,^a Taylor L. Weiss,^{‡b} Hem R. Thapa,^b Timothy P. Devarenne^{*b} and Arum Han^{*ac}

Microalgae are envisioned as a future source of renewable oil. The feasibility of producing high-value biomolecules from microalgae is strongly dependent on developing strains with increased productivity and environmental tolerance, understanding algal gene regulation, and optimizing growth conditions for higher production of target molecules. We present a high-throughput microfluidic microalgal photobioreactor array capable of applying 64 different light conditions to arrays of microscale algal photobioreactors and apply this device to investigate how light conditions influence algal growth and oil production. Using the green colony-forming microalga *Botryococcus braunii*, the light intensity and light–dark cycle conditions were identified that induced 1.8-fold higher oil accumulation over the typically used culture conditions. Additionally, the studies revealed that the condition under which maximum oil production occurs is significantly different from that of maximum growth. This screening test was accomplished using the developed photobioreactor array at 250 times higher throughput compared to conventional flask-scale photobioreactors.

 Received 17th December 2013,
Accepted 23rd January 2014

DOI: 10.1039/c3lc51396c

www.rsc.org/loc

Introduction

Microalgae have been envisioned as a future source of renewable oil for the production of transportation fuels.^{1–3} To produce enough microalgal oil to satisfy fuel demand (*i.e.*, to be commercially viable), it is necessary to develop better oil-producing strains through genetic and metabolic engineering or evolutionary pressure, to improve large-scale cultivation based on understanding of microalgal biology, to improve oil extraction methods, and to optimize the culture environment.

Current microalgal studies are conducted by culturing the organism in lab-scale flasks, open raceway ponds, or closed photobioreactors.^{1–4} These culture systems have made significant contributions to the understanding of basic algal biology, selecting the best strains for the production of biochemicals, and understanding the effects of various culture factors (*e.g.*, light intensity, light cycle, temperature, nutrient concentration, CO₂, pH) on algal

growth and oil production.⁴ However a clear understanding of the relationships between oil production and biomass increase in response to these various culture conditions for a variety of algae is still needed. There are two factors hampering these efforts. First, the light intensity and cycle exposed to each microalga changes as microalgal density increases over time in conventional photobioreactors, making it difficult to apply identical conditions to all microalgae in a given culture system for direct side by side comparison. Second, conventional flask-type photobioreactors are inadequate as high-throughput screening systems. The workload created by the combinatorial nature of many culture factors and the numerous microalgal strains to be considered, both natural and engineered, cannot be approached by simply doubling or tripling the throughput of currently available culture systems. Thus, a high-throughput photobioreactor array that can provide well-controlled culture conditions as well as quickly screen through various culture conditions to identify the best algal strains and conditions for fast growth and high oil production could significantly advance the current state of algal biofuel production.

Microfluidic lab-on-a-chip systems with their capability to precisely control, monitor and manipulate samples at the nano- to pico-liter scales as well as to integrate various steps in a particular biological assay are ideal for creating a high-throughput screening platform.^{5–7} A few microsystems for characterizing and distinguishing microalgal species have been reported,^{8–13} but they were simply analytic devices that lacked cell culturing capability. Microfluidic culture systems to examine microalgal

^a Department of Electrical and Computer Engineering, Texas A&M University, College Station, Texas 77843, USA. E-mail: arum.han@ece.tamu.edu

^b Department of Biochemistry and Biophysics, Texas A&M University, College Station, Texas 77843, USA. E-mail: tpd8@tamu.edu

^c Department of Biomedical Engineering, Texas A&M University, College Station, Texas 77843, USA

† Electronic supplementary information (ESI) available. See DOI: 10.1039/c3lc51396c

‡ Current address: Department of Biology, Washington University, Saint Louis, Missouri 63130, USA.

lipid production, density changes, or growth kinetics have also been developed.^{14–17} However, these systems could provide only a single culture environment at a time, not suitable for high-throughput screening applications. Recently, a high-throughput optical microplate-based culture platform was developed where growth and lipid production of microalgae under different light conditions could be studied.¹⁸ However it only allowed population-based studies, and long-term analysis was challenging due to the lack of nutrient supply capability. Single-cell/colony level studies will be crucial for developing better performing algal strains with characteristics such as fast growth rates, high oil production, and low levels of photoinhibition.

The high-throughput photobioreactor array presented here addresses the significant shortcomings of previous systems by providing single-colony resolution for photosynthetic micro-organism under an extremely well controlled environment at high throughput. The array is composed of a dynamic light controllable cell culture array capable of simultaneously studying the effect of 64 different light exposure conditions on algal growth and oil production with single-colony resolution. Coupled with arrays of 64 miniaturized microalgal culture chambers, 64 independent photobioreactor experiments could be conducted in parallel on a $5 \times 7 \text{ cm}^2$ footprint. Continuous perfusion of nutrient to each of the miniaturized photobioreactors having arrays of single-colony trapping microstructures allowed time-course analysis of algal growth and oil production over long periods of time. *Botryococcus braunii* is a green colonial microalga with significantly higher oil content compared to other microalgae.^{19,20} *B. braunii* race B produces hydrocarbon triterpene oils known as botryococcenes, which are attractive

because they can be easily converted into fuels suitable for internal combustion engines, including the petroleum-equivalent products such as gasoline, diesel, and kerosene using a single chemical process (hydrocracking).^{21,22} Thus, *B. braunii* race B, Berkeley strain was selected as our model microalga and its growth and oil accumulation under different light conditions were characterized with the developed microfluidic platform as a demonstration case.

Materials and methods

A high-throughput microfluidic microalgal photobioreactor array design

The microfluidic microalgal photobioreactor array is composed of four poly(dimethylsiloxane) (PDMS) layers stacked on top of each other (size: $5 \times 7 \text{ cm}^2$): a culture layer, a light intensity control layer, a light-dark cycle control layer, and a light blocking layer (Fig. 1A). The bottom microalgae culture layer has 64 culture compartments (diameter: $900 \mu\text{m}$, height: $85 \mu\text{m}$) connected to an inlet and an outlet through which microalgae and fresh media is introduced and waste is flushed out, respectively (Fig. 1B). Five single-colony trapping structures in the culture compartments enable the capture, culture, and analysis of microalgae with single-colony resolution over long periods of time (opening of each trap: $77 \mu\text{m}$, Fig. 1B–C). The light intensity control layer employs a microfluidic gradient generator to provide various intensities on a single platform with a single light source. The gradient generator utilizes a series of diffusive-mixing channel networks through which different dilutions of chemicals are automatically generated at outlets from two fluid

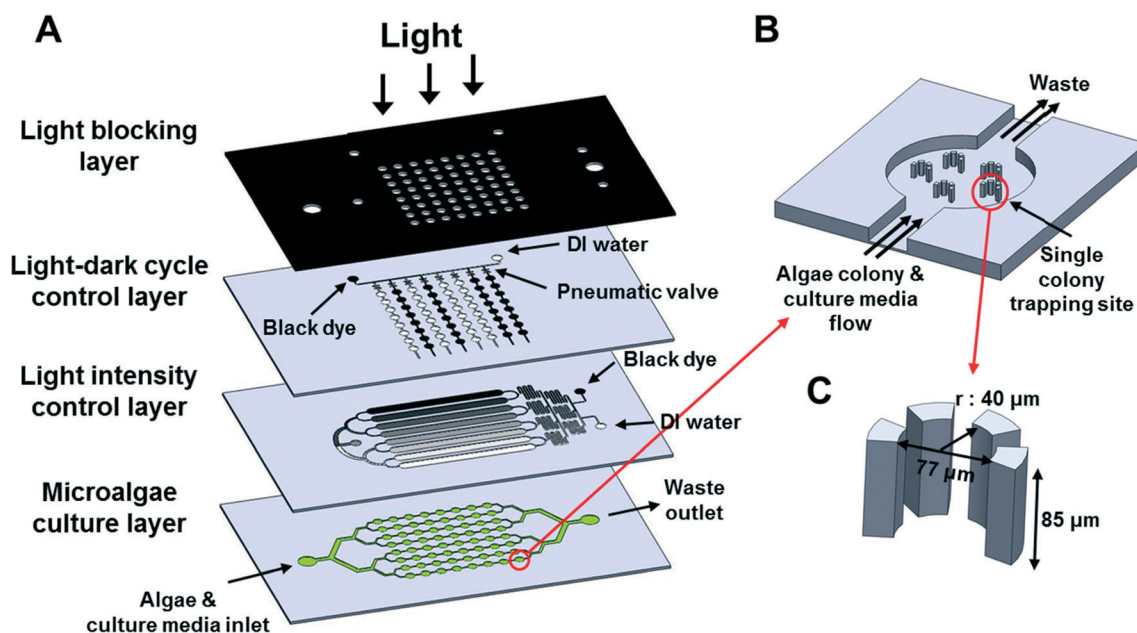


Fig. 1 The high-throughput microfluidic microalgal photobioreactor array. (A) The platform was composed of four layers – a light blocking layer, a microfluidic light-dark cycle control layer, a microfluidic light intensity control layer, and a microalgae culture layer. (B) Enlarged view of a single culture compartment having five single-colony trapping sites. (C) A single-colony trapping site composed of four micropillars.

inlets.^{23,24} By flowing deionized (DI) water and black dye through each inlet, the 8-outlet gradient generator produces 8 different concentrations of black dye into downstream channels. When a single light source is placed on top of these 8 channels, the different concentrations of black dye result in 8 different ranges of light shading effects to the underlying microalgae culture layer (Fig. 1A). The control of light–dark cycles is based on selectively filling each microfluidic channel in the light–dark cycle control layer either with DI water or black dye. When a channel is filled with DI water, 100% of light is transmitted to the underlying culture compartments, resulting in light (or “day”) condition. On the other hand, when a channel is filled with black dye, no light is transmitted, creating dark (or “night”) condition (Fig. 1A). Integrated pneumatic microvalve structures and a microfluidic binary demultiplexer (ESI†) are utilized to individually manage each of the 8 light–dark cycle control channels.²⁵ This enables switching between DI water (light) and black dye (dark) in a particular channel without affecting the light–dark cycles of other channels. Eight different light–dark cycles can be implemented by periodically filling each channel with either DI water or black dye at 8 different time periods. To screen microalgae against 64 different light conditions in parallel, the 8 light intensity control channels and the 8 light–dark cycle control channels are placed perpendicular to each other for generating 64 unique light conditions to the 64 microalgal culture compartments underneath (Fig. 1A). The top light blocking layer in the microfluidic platform is employed to provide isolated light conditions onto each of the underlying microalgae culture compartments. The overall operation of the systems is visualized in ESI† video S1.

Microfluidic microalgae photobioreactor array fabrication

The multi-layer microfluidic photobioreactor array was fabricated in PDMS using soft-lithography, a method where hundreds of polymer replicas can be stamped out from a single master mold.²⁶ The top light blocking layer was made by replicating a black-color PDMS layer (Sylgard® 170, Dow Corning, Inc., Midland, MI) from CNC-machined acrylic masters (12.5 mm, McMaster-Carr, Atlanta, GA) for blocking all light except for openings for the microalgae culture area and the inlet/outlet interface area.

The master molds for the light intensity control layer, the light–dark cycle control layer, and the microalgae culture layer were all fabricated with photosensitive epoxy (SU-8™, Microchem, Inc., Newton, MA) using a conventional photolithography process. The microfluidic gradient generator channels in the light intensity control layer and the light–dark cycle control channels in the light–dark cycle control layer were 90 μm thick, and the master molds were fabricated by spin-coating SU-8™ 2075 at 1950 rpm. The pneumatic binary demultiplexer in the light–dark cycle control layer was 150 μm thick, and the master mold was obtained by spin-coating SU-8™ 2075 at 1000 rpm. These three masters were soft-baked at 65 °C for 24 hours, followed by another soft-baking step at 95 °C for 40 minutes. The master mold for the microalgae culture layer, 85 μm thick, was patterned with SU-8™ 2050 by spin-coating at 1500 rpm

and soft-baking in two steps at 65 °C and 95 °C for 60 and 20 minutes, respectively. All masters were exposed to ultraviolet (UV) light followed by a two-step post-exposure baking at 65 °C for 10 minutes and at 95 °C for 20 minutes. Before PDMS replication, all SU-8™ master molds were coated with a surfactant, (tridecafluoro-1,1,2,2-tetrahydrooctyl) trichlorosilane (United Chemical Technologies, Inc., Bristol, PA), to facilitate PDMS release without damaging the master molds, followed by rinsing with isopropyl alcohol (IPA) to remove excessive coating residues.

PDMS layers forming the microfluidic gradient generator channels and the light–dark cycle control channels (both 130 μm thick) and the pneumatic binary demultiplexer (300 μm thick PDMS) were replicated from the SU-8™ masters by spin-coating 8 g of PDMS pre-polymer at the speed of 700 rpm and 300 rpm for 40 seconds, respectively. To create the high-aspect-ratio trapping structures (85 μm/25 μm = 3.4) in the PDMS microalgae culture layer, an SU-8™ master mold having corresponding high-aspect-ratio holes are required. However, a two-step PDMS casting method with a SU-8™ master having raised trapping structures was utilized rather than a typical single-layer casting method that resulted in severe crack to the structure due to the very long developing process. First, a PDMS master having deep holes was cast from the SU-8™ master by pouring 7 g of PDMS pre-polymer and curing it at 85 °C for 3 hours. The PDMS master was then coated with trichlorosilane and rinsed with IPA. A PDMS microalgae culture layer (around 300 μm thick) having the same features with the SU-8™ master was replicated from the PDMS master by pouring 2.5 g of PDMS pre-polymer and curing it at 85 °C for 4 hours.

All PDMS layers were treated with oxygen plasma (Plasma cleaner, Harrick Plasma, Ithaca, NY) before assembly. This PDMS assembly forming the microfluidic microalgal photobioreactor array was then bonded with an acrylic frame, which provided a CO₂-controlled environment required for microalgae culture. The overall fabrication steps and assembly processes are summarized in ESI† Fig. S1.

Light intensity measurement

To characterize light transmission through different concentrations of black dye (different shading effects depending on black dye concentrations), light intensities penetrating through the light intensity control layer were measured using a quantum sensor (LI-190 Quantum Sensor with LI-250A Light Meter, LI-COR Bioscience, Lincoln, Nebraska). A light intensity control layer having 90 μm deep microfluidic channels was utilized to measure 19 different black dye (black ink kit for Epson 78 printer) concentrations (0, 0.3, 0.5, 1, 1.5, 2, 2.5, 3.5, 4, 5, 6.5, 8.5, 10, 15, 20, 40, 60, 80, 100%). A 14-W compact fluorescent light bulb (65 K) was placed on top as a light source, and the transmitted light intensity was measured by first changing the concentration of black dye inside the light intensity control channels and then by changing the distance between the device and the light source (from 4.5 cm to 25 cm) to control the maximum light intensity.

The light blocking layer in the microfluidic platform was employed to provide isolated light conditions onto each of the underlying microalgae culture compartments. To validate this capability, all open chambers in the light blocking layer were blocked except for one chamber (highlighted as “Open” in ESI† Fig. S2A) to which light could penetrate. The intensities of light underneath the open chamber as well as adjacent blocked chambers were measured using the quantum sensor, and these measured intensities were compared to examine whether the light passing through the open chamber affected the neighboring chambers. The measurements were conducted at a light intensity of $165 \mu\text{mol photons m}^{-2} \text{s}^{-1}$ by changing the distance between the light blocking layer and the quantum sensor, from 0.5 to 1.5 mm, corresponding to the gap between the microalgae culture layer and the light blocking layer (ESI† Fig. S2B).

Preparation of *Botryococcus braunii*

Prior to loading into the microfluidic platform, *B. braunii* race B, Berkeley (or Showa) strain²⁷ was cultured in 800 ml of modified Chu 13 media,²⁸ grown under 13-W compact fluorescent (65 K) lighting at a distance of 9.5 cm, which results in a light intensity of $80 \mu\text{mol photons m}^{-2} \text{s}^{-1}$. The cultures went through a 12 hour light–dark cycle at 22.5 °C, and were continuously aerated with filter-sterilized air containing 2.5% CO₂. Subsequent subcultures were conducted every 4 to 6 weeks by inoculating 750 ml of new media with 50 ml of mature culture.^{29,30} *B. braunii* in rapid growth phase (6–8 days after every subculture) were collected and used for analysis in the microfluidic platform.

B. braunii culture inside the microfluidic microalgal photobioreactor array

The microfluidic platform was sterilized with UV light for at least one hour prior to a culture experiment. The microalgae culture layer and the light intensity/cycle control layers were flushed with culture media and DI water, respectively. *B. braunii* loading was performed with a syringe pump (Fusion 200, Chemx Inc., Stafford, TX, $1\text{--}3 \mu\text{l min}^{-1}$). Once *B. braunii* colonies were loaded and captured at all of the trapping sites, any excessive algae that were not captured by the trapping sites were flushed out with culture media ($10\text{--}15 \mu\text{l min}^{-1}$ for 10 minutes). During the culture, the platform was placed under a single light source at a distance of 9.7 cm ($132 \mu\text{mol photons m}^{-2} \text{s}^{-1}$) for the 16 different light intensity condition experiments and at 10.7 cm ($120 \mu\text{mol photons m}^{-2} \text{s}^{-1}$) for the 8 different light–dark cycle condition experiments. Fresh culture media was continuously perfused with the syringe pump at a flow rate of $1 \mu\text{l min}^{-1}$, and 2.5% CO₂ enriched air was provided at a flow rate of 500 ml min^{-1} to the acrylic frame holding the microfluidic platform. Since PDMS is gas permeable,³¹ the gas concentration inside the microfluidic platform is identical to the gas concentration inside the acrylic frame. The entire operation of the system is automatically controlled by a Labview™ interface controlling syringe pumps and pneumatic solenoid valves. The overall experimental setup is illustrated in ESI† Fig. S3.

Growth analysis

Growth of *B. braunii* inside the microfluidic platform was characterized by tracking the sizes of colonies captured in each of the trapping sites over time. Immediately after the cell loading process, all *B. braunii* were imaged using an Eclipse TS 100F microscope (Nikon Instruments, Inc.) equipped with a digital camera (DS-2MV), and these images were used as references (day 0). Once the culture started, images were taken every 2–3 days. To quantify the size change, the size of each *B. braunii* colony was first analyzed with an image analysis software package (Image J) by measuring its area. Then, the sizes of *B. braunii* colonies were compared to its initial size to characterize the growth. The single-colony trapping site allowed time-lapse imaging of the exactly same colony over the entire culture period, providing single-colony resolution growth data. At least 18 and 15 different samples were analyzed to obtain growth data for the 16 different light intensity and the 8 different light–dark cycle experiments, respectively.

The chlorophyll autofluorescence of *B. braunii* colonies captured inside the microfluidic platform was also characterized to analyze the relationship between the colony sizes and fluorescence intensities. Microscopy for quantifying chlorophyll autofluorescence was conducted using a Zeiss Axio Observer Z1 microscope (Carl Zeiss MicroImaging, LLC) equipped with a digital camera (Orca Flash2.8 CMOS Camera) and a filter set (excitation: 460–500 nm, emission > 600 nm). The size of *B. braunii* and its corresponding intensity sum of chlorophyll autofluorescence were measured using an image analysis software (Image J), and the correlation between these measurements was analyzed (ESI† Fig. S4).

Quantifying oil production

To analyze and quantify the amount of oil accumulated by *B. braunii* under different light conditions, Nile red fluorescence staining was utilized. Nile red, a lipid-soluble fluorescent dye that binds to neutral lipids, has been shown to efficiently stain *B. braunii* oil in the extracellular matrix as well as in intracellular oil bodies,^{29,30} and has been used to accurately evaluate the oil content in *B. braunii*.^{32,33} It has been also reported that the fluorescence intensity of cells stained with Nile red and the lipid content in *B. braunii* determined by a conventional solvent extraction system shows a linear relationship ($R^2 = 0.998$).³³ Thus, in our microfluidic microalgae platform, the oil amount in *B. braunii* was analyzed by staining with Nile red and estimating the oil content based on the fluorescent intensity.

However, due to PDMS absorbing hydrophobic small molecules, Nile red staining inside the PDMS microalgae platform can cause severe background fluorescence.³⁴ To resolve this issue, the PDMS platform was first filled with 3% Bovine Serum Albumin (BSA) and incubated at room temperature for 3–5 hours, followed by rinsing with culture media. For oil content measurement both before and after the culture period, a Nile red solution in acetone was diluted in culture media to a concentration of $0.75 \mu\text{g ml}^{-1}$ Nile red and 0.5% acetone, and this diluted solution was flowed through the culture

chambers where microalgae were captured for 1 hour at a flow rate of $1\text{--}10\ \mu\text{l min}^{-1}$. The channels were then rinsed with fresh culture medium for 10 minutes.

An alternative method is to selectively extract desired microalgal colonies off-chip for Nile red staining and oil quantitation. By applying a backflow to the culture compartment, *B. braunii* colonies that were captured inside the trapping sites could be sequentially released and collected to off-chip reservoirs and then stained with Nile red. This process still allowed us to trace a specific colony to its original position due to the sequential nature of the release process into off-chip reservoirs. Even though this protocol was more time-consuming than on-chip staining, it ensured that all colonies were exposed to the same amount of Nile red solution, thus minimizing potential fluorescence intensity variations due to different degree of Nile red staining. Thus, this protocol was used to obtain accumulated oil data as well as oil per unit area data in the result section. We are currently in the process of fully characterizing various on-chip staining protocols to minimize such potential variations.

After Nile red staining, microscopic images were obtained using a Zeiss Axio Observer Z1 microscope equipped with a digital camera (Orca Flash2.8 CMOS Camera) and a filter set (excitation: 450–490 nm, emission: 500–550 nm). To characterize the oil per unit area in *B. braunii*, first, Nile red fluorescence intensity per unit area of each *B. braunii* colony was measured using the Image J software, and then compared to the value measured at day 0. The increase in overall oil amount accumulated during the culture was also analyzed by calculating the ratio of the initial oil amount (initial *B. braunii* size \times fluorescence intensity per unit area measured at day 0) and the final oil amount (final *B. braunii* size \times fluorescence intensity per unit area measured at the end of the culture). At least 23 and 21 different samples were analyzed to obtain oil data for the 16 different light intensity and the 8 different light–dark cycle experiments, respectively.

Results

Single microalga colony trapping

Single-colony trapping structures in the culture compartments, each consisting of 4 standing pillars with a gap between them, allowed the capture, culture, and analysis of microalgae with single-colony resolution over long periods of time (Fig. 1B–C, ESI† S5C). During the cell loading process, *B. braunii* suspended in culture media was flowed into the platform and the colonies were hydrodynamically captured by the trapping sites. Owing to the gaps and a slightly larger opening size ($77\ \mu\text{m}$) of the trapping site compared to *B. braunii* colony size (Berkeley strain, typical diameter: $50\text{--}70\ \mu\text{m}$), single colonies could be successfully captured (Fig. 2A). Efficiency of fully occupying all trapping sites with *B. braunii* was $98.4 \pm 1.1\%$ (315 out of 320 trapping sites on a single device). Since captured colonies could not escape the trapping sites under continuous perfusion, continual monitoring of the same *B. braunii* throughout a long-term culture was possible. As the microfluidic platform is compatible with light and fluorescence microscopy, algal colonies captured inside the trap could be analyzed in real-time by examining their growth based on bright-field imaging (Fig. 2A) and Nile red-based fluorescence imaging (Fig. 2C) for quantifying biomass and oil production, respectively.

Microfluidic control of light intensity

The microfluidic gradient generator was utilized in the light intensity control layer to generate various intensities of light on a single platform with a single light source. First, a 16-outlet gradient generator was employed instead of the 8-outlet design to characterize the relationship between the concentrations of black dye and resulting light intensities (Fig. 3A). Stronger light intensities (*i.e.*, higher light transmissions) were observed as the concentration of black dye dropped and the distance between the light source and the platform became closer

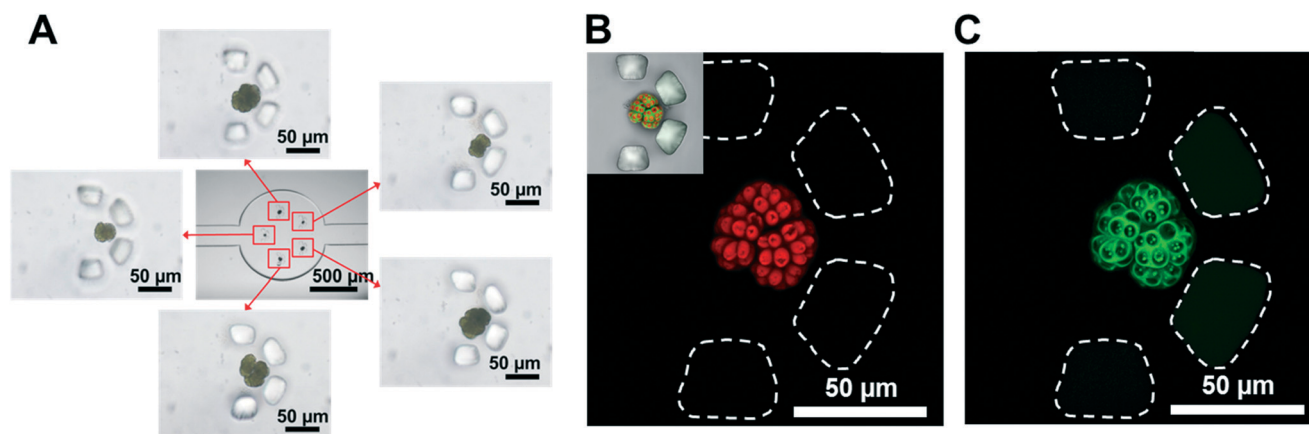


Fig. 2 Single *B. braunii* colony trapping in the microfluidic photobioreactor array. (A) A single microalgal cultivation compartment where five *B. braunii* colonies were captured inside each of the trapping sites. (B) Chlorophyll autofluorescence and (C) lipid-stained images (through Nile red treatment) of a single *B. braunii* colony inside the trapping structure. Inset shows merged image of corresponding bright-field, chlorophyll autofluorescence, and Nile red fluorescence. Dotted lines indicate micropillar structures that formed a single trapping site.

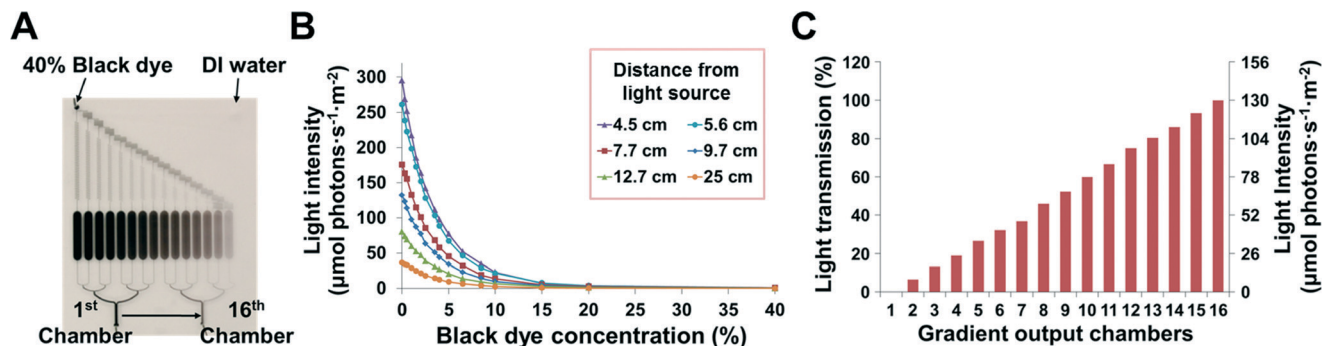


Fig. 3 On-chip control of light intensity. (A) Light intensity control layer producing 16 different concentrations of black dye through the microfluidic gradient generator, where DI water (flow rate: $0.8 \mu\text{L min}^{-1}$) and 40% black dye (flow rate: $5 \mu\text{L min}^{-1}$) were used as the two inputs. (B) Correlation between measured light intensities and black dye concentrations. Distances between the light source and the platform were adjusted to control the incident light intensity. (C) Corresponding transmitted light intensities showing 16 different light intensities within a single microfluidic platform.

(Fig. 3B, ESI† Table S1). When a particular concentration of black dye was filled in the channel, regardless of the intensity of the light source, the transmission rate through the particular black dye concentration was almost consistent (less than 2% standard deviations for each black dye concentration from 6 different incident light intensities, ESI† Table S1). Thus, each row of the culture compartments in the underlying microalgae culture layer was exposed to one of the 16 light intensities generated. The gradient generator was designed so that a linear range of light intensities can be generated (Fig. 3C, generated transmission rate from 0% to 100% ($R^2 = 0.9991$), corresponding to 0 – $132 \mu\text{mol photons m}^{-2} \text{s}^{-1}$). The absolute light intensity on this platform can be easily changed, if needed, by simply adjusting the input black dye concentrations or the distance between the light source and the platform. When the light intensity control layer was used in combination with the light–dark cycle control layer, the 8-outlet gradient generator was used instead of the 16-output design (ESI† Fig. S5B).

Microfluidic control of light–dark cycles

Light (or “day”) and dark (or “night”) conditions in the light–dark cycle control layer were realized by filling each channel with DI water and black dye, respectively. The intensities of transmitted light through DI water- and black dye-filled channels (height: $90 \mu\text{m}$) in the light–dark cycle control layer were measured, and 100% and 0% transmissions were confirmed. The pneumatic binary demultiplexer successfully controlled the light–dark cycles in each of the 8 control channels independently (Fig. 4A–C), resulting in 8 different light–dark cycles on-chip; 2, 4, 6, 8, 10, 12, 16, and 24 hours (Fig. 4D). A 2 hour cycle means switching between light and dark conditions every 2 hours.

The transition time to switch between DI water (light) and black dye (dark), which determines the shortest possible light–dark cycle in the platform, could be easily adjusted by changing the flow rate of the two solutions. For example, at a flow rate of $1.5 \mu\text{L min}^{-1}$, the transition time was less than 4 minutes, and at a flow rate of $3.0 \mu\text{L min}^{-1}$, the transition time was less than 2 minutes, which is the fastest possible transition time under these conditions. During all culture experiments presented here, the flow rate was set to $1.5 \mu\text{L min}^{-1}$.

Isolation of light conditions

By creating 64 circular open chambers smaller than both the light–dark cycle and the light intensity control channel widths, the top light blocking layer was successfully utilized to prevent any light that was not passing through both the light–dark cycle and the light intensity control layers from reaching the underlying microalgae culture layer (ESI† Fig. S5A). This layer also isolates the light conditions between chambers by blocking potential scattered light from neighboring chambers. A negligible amount of light interference between adjacent chambers (less than 1.5%) was observed (ESI† Fig. S2).

Analysis of microalgal growth and oil production under different light intensities

B. braunii colonies in the microfluidic platform were cultured for 12 days under 16 different light intensities (Fig. 3C), all under a 12 hour light–dark cycle (*i.e.*, 12 h light and 12 h dark), to study the effect of light intensity on growth and oil production. The growth of *B. braunii* was characterized by tracking its size changes over time, where the size was analyzed by measuring the area of each colony. Nile red fluorescence staining was utilized to monitor and quantify oil (botryococenes) content. Oil per unit area from each colony was defined as Nile red fluorescence intensity per unit area, and the total oil amount accumulated inside a colony was quantified by multiplying the colony size and the oil per unit area. Time-lapse microscopy showed that different light intensities resulted in different size increases (Fig. 5A) and analysis of Nile red stained *B. braunii* also showed differences in oil accumulation under varying light intensities (Fig. 5B).

The average colony size increase under the 12 hour cycle after 12 days of growth increased up to a certain light intensity level (229% increase at $113 \mu\text{mol photons m}^{-2} \text{s}^{-1}$), but then showed a lower size increase as light intensity increased (171% increase at $132 \mu\text{mol photons m}^{-2} \text{s}^{-1}$, Fig. 5C), compared to day 0, possibly due to photoinhibition. The trend in size increase under different light intensities was similar throughout the time-course experiment (5, 7, 10, and 12 days of culture) (ESI† Fig. S6). This growth trend indicates that culture periods

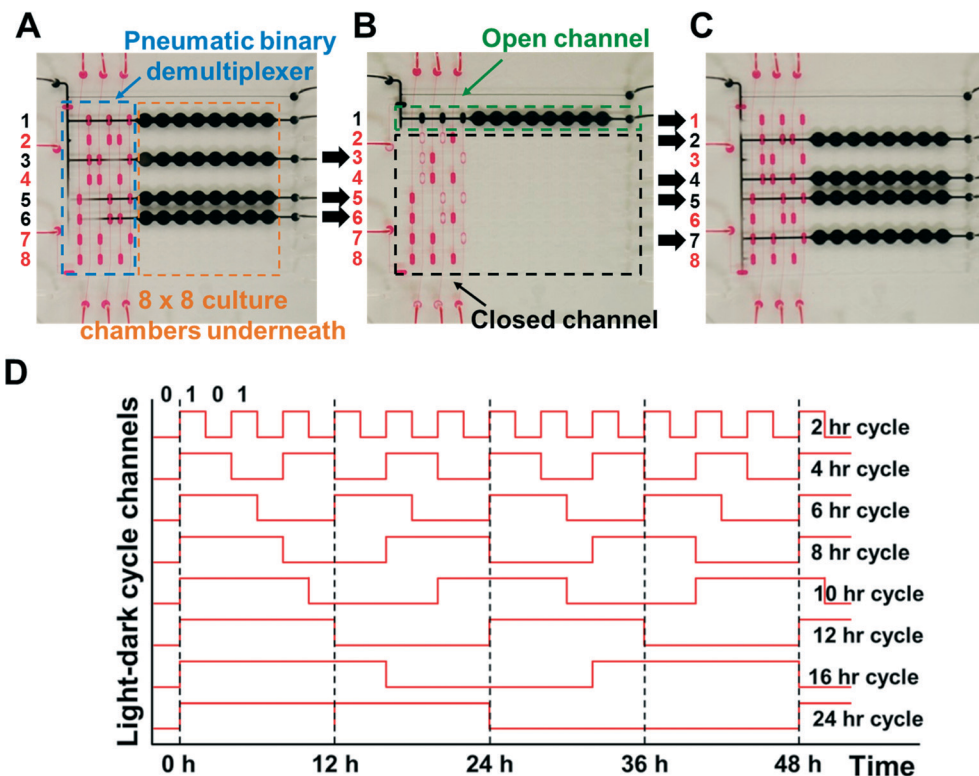


Fig. 4 Operation of the microfluidically actuated light–dark cycle control layer. Channels labeled 1–8 indicate the 8 individual light–dark cycle control channels controlled by a pneumatic binary demultiplexer. Black and red lettering indicates black dye and DI water filled channels, respectively. (A) Channels 1, 3, 5, and 6 filled with black dye, resulting in a “dark” cycle to the underlying culture chambers, while channels 2, 4, 7, and 8 filled with DI water resulting in a “light” cycle. (B) Only channel 1 in a “dark” cycle. (C) Culture chambers under channels 2, 4, 5, and 7 going through a “dark” cycle, while the rest of the chambers going through a “light” cycle. (D) Eight different light–dark cycles used in the subsequent experiments.

between 10 and 12 days may be sufficient to evaluate the effects of light intensity on the growth characteristics of *B. braunii*.

Oil per unit area became higher as the light intensity increased (maximum increase: 51 % compared to day 0), but then started to plateau or slightly decrease as the light intensity was raised ($99 \mu\text{mol photons m}^{-2} \text{s}^{-1}$ and higher, Fig. 5D). Interestingly, maximum oil per unit area was observed at a slightly lower light intensity level ($99 \mu\text{mol photons m}^{-2} \text{s}^{-1}$, Fig. 5D) compared to the intensity under which maximum size increase was observed ($113 \mu\text{mol photons m}^{-2} \text{s}^{-1}$, Fig. 5C). Thus, even at a light intensity under which maximum size increase was observed, oil production per unit area seems to have already saturated, possibly due to the stress response to increased light intensity. However, maximum total oil accumulation during culturing still occurred under the same light intensity that produced the maximum size increase ($113 \mu\text{mol photons m}^{-2} \text{s}^{-1}$, Fig. 5C).

Analysis of microalgal growth and oil production under different light–dark cycles

To investigate the effect of different light–dark cycles on growth and oil production, *B. braunii* colonies in the microfluidic platform were cultured under 8 different cycles (2, 4, 6, 8, 10, 12, 16, and 24 hours of day and night) for 17 days at a light intensity of $120 \mu\text{mol photons m}^{-2} \text{s}^{-1}$ (Fig. 6A–B). The light

intensity of $120 \mu\text{mol photons m}^{-2} \text{s}^{-1}$ was selected since that intensity was close to the level where maximum growth and oil accumulation was observed (Fig. 5C). Over a 17 day analysis, the colony size increase compared to day 0 peaked under the 8 hour cycle at 191%, and then rapidly dropped to about a 148% increase under the 12 hour cycle (Fig. 6C), a light cycle commonly used in conventional *B. braunii* cultures.^{29,30,35} The size increase further dropped to a 108% increase at the 24 hour cycle (Fig. 6C). Further time-course analyses of size increase after 4, 7, 11, and 14 days of culture period showed that a similar trend was observed after 11 days of culturing (ESI† Fig. S7). Combined with our light intensity studies above that showed an optimal culturing period of 10–12 days, the 11 day time point should be sufficient to fully understand the growth characteristics of *B. braunii*, a tremendous reduction in time compared to the conventional 4–6 week laboratory-scale culture.^{29,30,35}

The highest amount of oil per unit area was observed under the 2 hour cycle (45% increase compared to day 0), 1.8 times higher compared to the oil per unit area under the typically used 12 hour cycle (25% increase compared to day 0, Fig. 6D). Interestingly, maximum total oil accumulation was observed under the 8 hour cycle (261% increase compared to day 0, Fig. 6C), the same condition under which the largest colony size increase was observed (Fig. 6C). However, due to the significantly higher oil production per unit area (Fig. 6D), total oil accumulation

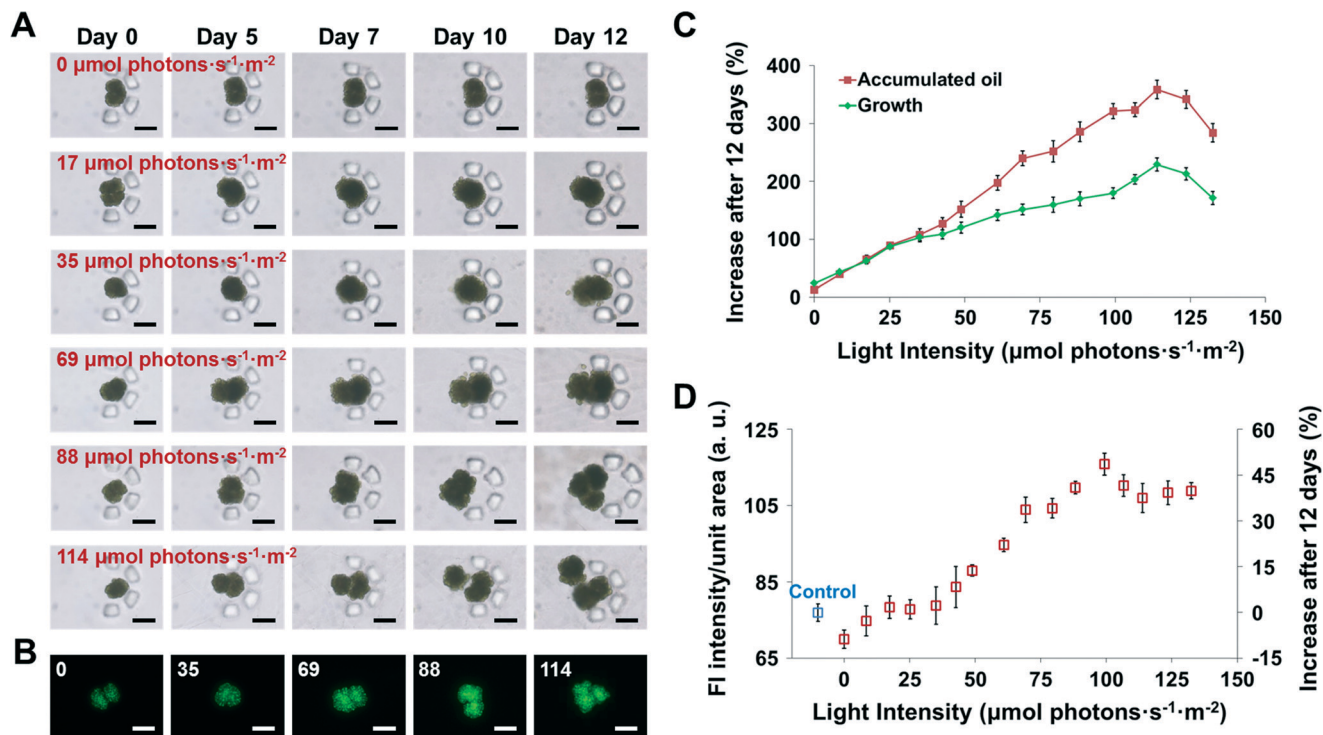


Fig. 5 Analysis of *B. braunii* growth and oil production under 16 different light intensities with a 12 hour light–dark cycle. (A) Example images of *B. braunii* colonies at days 0, 5, 7, 10, and 12 from six of the 16 light intensities used. (B) Example images of *B. braunii* colonies stained with Nile red after 12 days of culture. The number in each image indicates light intensity. (C) Increase in average *B. braunii* colony size and oil amount after 12 days of culture under 16 different light intensities ($n = 18$). (D) Average oil per unit area (Nile red fluorescence intensity per unit area) in *B. braunii* after 12 days of culture ($n = 23$). Control indicates the average oil per unit area measured at day 0. All data shown are mean \pm standard error. Scale bar = 50 μm .

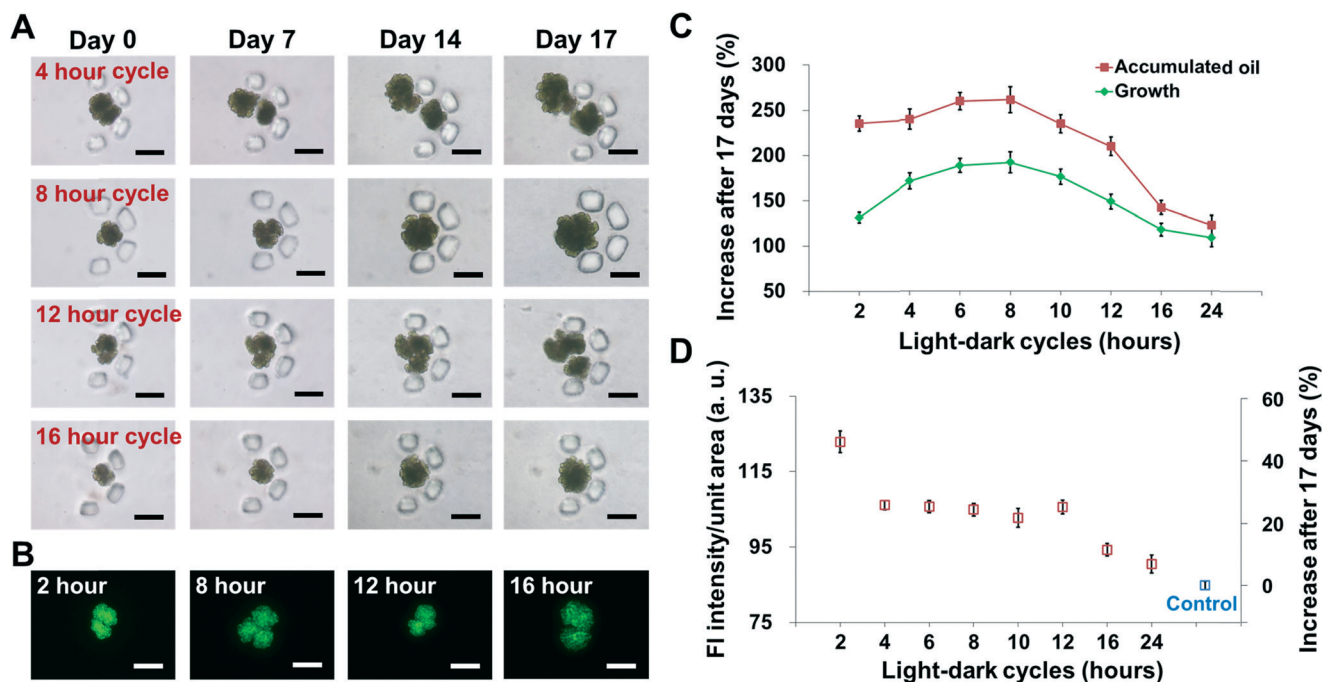


Fig. 6 Analysis of *B. braunii* growth and oil production under 8 different light–dark cycles at a light intensity of $120 \mu\text{mol photons m}^{-2} \text{ s}^{-1}$. (A) Example images of single *B. braunii* colonies at day 0, 7, 14, and 17 days. (B) Example images of *B. braunii* colonies stained with Nile red after 17 days of culture. (C) Increase in average size and oil amount after 17 days ($n = 15$). (D) Average oil per unit area in *B. braunii* after 17 days ($n = 21$). Control indicates the average oil per unit area measured at day 0. All data shown are mean \pm standard error. Scale bar = 50 μm .

under the 2, 4, and 6 hour cycles all showed relatively high increases compared to day 0 (235, 239, and 259% increase, respectively, Fig. 6C). The use of our photobioreactor array allowed us to define the conditions to optimize oil production (per unit area and total accumulation) compared to the currently used culture conditions, and more importantly this device will allow for future detailed mechanistic studies to be conducted for direct side-by-side comparisons between growth and oil production for a wide variety of algal strains of interest.

Discussion

We have demonstrated a high-throughput microfluidic microalgal photobioreactor array capable of investigating the effect of 64 different light conditions on microalgal growth and oil production. Continuous perfusion of nutrients to each culture compartment containing multiple single-colony trapping structures allowed long-term analysis with single-colony resolution. This platform also overcame the limitations of conventional culture systems by applying identical conditions to all microalgae in trapping sites and implementing high-throughput screening capabilities.

As most microalgae obtain their metabolic energy from photosynthesis, microalgal growth and oil production are strongly dependent on light conditions. Different growth/biomass increases and oil production have been reported under different light intensities and cycles.^{36–38} In particular, different ranges of favorable light intensity and cycles for improved growth/biomass increase and oil production have been studied for the different strains of *B. braunii*.^{19,20,39,40} However, the favorable light conditions even for a single *B. braunii* strain can differ depending on culture systems, which makes it challenging to compare the significance of the relationship between light conditions and growth/oil production amongst these previous studies.^{29,30,35,41} This might result from the different culture systems used for testing and the lack of tools applicable for examining the relationship at a microscopic level, which our microfluidic photobioreactor array overcomes.

Growth and oil production for *B. braunii* under different light intensities and cycles were successfully characterized using the developed platform. The trends of growth and oil production observed from different light conditions matched well with recent research,⁴¹ where increasing growth rate was observed with increasing light intensity, but then decreased beyond a specific light intensity. In typical flask cultures, *B. braunii* biomass increase over a 12 day culture period has been reported to be 26%,³⁵ which is much lower to that observed under this microfluidic platform. It is also known that oil accumulation increase over a 12 day culture period is in the range of a 28% increase,³⁵ again much lower to that observed under this microfluidic platform. Thus, this platform may provide better growth conditions (more direct light exposure to the colony) over the standard culturing system. It has also been reported that a linear relationship exists between hydrocarbon content (oil amount) and growth rates.⁴¹ A similar

relationship was obtained from our platform where the highest oil accumulation was observed under the light condition that also showed maximum growth. Our study also shows a decrease in growth and oil production beyond the light intensity of $113 \mu\text{mol photons m}^{-2} \text{s}^{-1}$. While this level of light intensity may be low for photoinhibition compared to that seen in land plants, studies have shown that photoinhibition can occur even at low light levels and is related to the total irradiance received by the cell, not the amount of excess light.⁴² Additionally, photoinhibition in the green microalga *Neochloris oleoabundans* has been shown to occur at light levels above $180 \mu\text{mol photons m}^{-2} \text{s}^{-1}$, a level very similar to that presented in this study.⁴³ As a matter of fact, this finding of light level that causes photoinhibition in *B. braunii* has not been previously reported.

An interesting finding was that the 2 hour light–dark cycle showed higher oil production per unit area compared to the conventionally used 12 hour cycle (1.8 times). This was different from the 8 hour cycle under which maximum total oil accumulation and growth were observed. This was due to the fact that a high level of oil production per unit area occurred between the 2–6 hour cycles even though the growth for these cycles was slower than that of the 8 hour cycle. This finding clearly demonstrates the importance of fully understanding the relationship between growth and oil accumulation under combinations of different light intensities and light–dark cycles.

The growth and oil production studies conducted through the microfluidic photobioreactor array here is meant to serve as a demonstration of a standardized photobioreactor platform that can be used to examine algal growth and oil production under a combination of different conditions. Additionally, the use of this device demonstrates that such detailed characterizations could be conducted for a large variety of different algal strains, both natural and engineered, at high throughput. We believe that this platform can be an ideal tool in developing better algal strains with increased oil production. The knowledge gained through such studies also has the potential to be directly utilized in large-scale cultures. For example, information on how light cycles influence algal growth and oil production can be used in optimizing conditions in large-scale outdoor cultures through artificial shading or in developing new indoor photobioreactors that can provide such optimum light cycles at a minimum cost.

Conventional *B. braunii* culture periods are very long (4–6 weeks)^{29,30,35} due to their slow growth rate, which makes analysis of optimal growth conditions very time-consuming. Therefore, *B. braunii* is a good model microalga for studying slow-growing microalgae as well as for assessing the long-term culture and analysis capabilities of the developed platform. In conventional flask culture systems, 800 ml of media is required to support 6 weeks of culturing *B. braunii* under a single light condition. However, in the microfluidic platform, 60.48 ml of media is needed to culture *B. braunii* for 6 weeks under 64 different light conditions (continuous media perfusion rate: $1 \mu\text{l min}^{-1}$, $1 \mu\text{l min}^{-1} \times 60 \text{ minutes} \times 24 \text{ hours} \times 42 \text{ days} = 60.48 \text{ ml}$), and thus, each light condition requires 945 μl of media ($60.48 \text{ ml}/64 = 945 \mu\text{l}$), almost 850 times

less reagent consumption compared to current conditions (800 ml/945 μ l = 846.6). More importantly, growth characteristics of *B. braunii* under 64 different light conditions can be analyzed after 11 days of culture inside the microfluidic platform, resulting in almost 250 times higher throughput (64 experiments/11 days \times 42 days = 244.4) compared to the conventional flask system (1 experiment/42 days).

The current platform utilizes arrays of single-colony trapping microstructures for the presented analysis. However, trapping structure design can be easily modified to accommodate different numbers of colonies (ESI† Fig. S8), which would enable studying the effect of different population densities on growth/biomass/oil production, which have been reported in some microalgae.^{44,45} The growth characteristics of algae in the current study were evaluated through size tracking using bright field microscopy, making automated image analysis challenging. Measurement of chlorophyll autofluorescence is one of the most widely used and convenient methods to estimate algal biomass.^{46,47} Our study shows that there is a strong correlation ($R^2 = 0.9937$) between the intensity sum of chlorophyll autofluorescence and the size of *B. braunii* (ESI† Fig. S4). This suggests that algal growth analysis can be conducted through fluorescent imaging in the future, which is much more amenable for fully automatic image processing to minimize the analysis time.

Conclusion

A high-throughput microfluidic microalgae photobioreactor array was developed to investigate growth and oil production of microalgae under 64 different light conditions with single-colony resolution, in parallel. *B. braunii* colonies were successfully characterized using the developed platform and resulted in identifying light conditions that showed maximum oil production that differed from conditions typically used in conventional cultures. This screening was achieved at 250 times higher throughput and 850 times less reagent consumption. We expect that this platform will serve as a powerful tool to investigate how algal growth and oil production are influenced by light conditions as well as screening through various growth conditions against algal strains of interest, all at significantly lower cost and shorter time, which can dramatically accelerate the development of renewable algal energy systems.

Acknowledgements

This work was supported by the National Science Foundation (NSF) Emerging Frontiers in Research and Innovation (EFRI) grant #1240478 to A.H. and T.P.D and by contract DE-EE0003046 awarded to the National Alliance for Advanced Biofuels and Bioproducts (NAABB, of which T.P.D is a member) from the U.S. Department of Energy. Any opinions, findings, and conclusions or recommendations expressed in this material are those of the author(s) and do not necessarily reflect the views of the National Science Foundation.

References

- 1 Y. Chisti, *Biotechnol. Adv.*, 2007, 25, 294–306.
- 2 Y. Chisti, *Trends Biotechnol.*, 2008, 26, 126–131.
- 3 D. R. Georgianna and S. P. Mayfield, *Nature*, 2012, 488, 329–335.
- 4 S. A. Scott, M. P. Davey, J. S. Dennis, I. Horst, C. J. Howe, D. J. Lea-Smith and A. G. Smith, *Curr. Opin. Biotechnol.*, 2010, 21, 277–286.
- 5 G. M. Whitesides, *Lab Chip*, 2011, 11, 191–193.
- 6 G. B. Salieb-Beugelaar, G. Simone, A. Arora, A. Philippi and A. Manz, *Anal. Chem.*, 2010, 82, 4848–4864.
- 7 D. Mark, S. Haeberle, G. Roth, F. von Stetten and R. Zengerle, *Chem. Soc. Rev.*, 2010, 39, 1153–1182.
- 8 A. Han, H. Hou, L. Li, H. S. Kim and P. de Figueiredo, *Trends Biotechnol.*, 2013, 31, 225–232.
- 9 A. Schaap, Y. Bellouard and T. Rohrlack, *Biomed. Opt. Express*, 2011, 2, 658–664.
- 10 N. Hashemi, J. S. Erickson, J. P. Golden and F. S. Ligler, *Biomicrofluidics*, 2011, 5, 032009.
- 11 A. Schaap, T. Rohrlack and Y. Bellouard, *Lab Chip*, 2012, 12, 1527–1532.
- 12 R. A. Erickson and R. Jimenez, *Lab Chip*, 2013, 13, 2893–2901.
- 13 D. H. Lee, C. Y. Bae, J. I. Han and J. K. Park, *Anal. Chem.*, 2013, 85, 8749–8756.
- 14 R. E. Holcomb, L. J. Mason, K. F. Reardon, D. M. Crokep and C. S. Henry, *Anal. Bioanal. Chem.*, 2011, 400, 245–253.
- 15 S. H. Au, S. C. Shih and A. R. Wheeler, *Biomed. Microdevices*, 2011, 13, 41–50.
- 16 J. Pan, A. L. Stephenson, E. Kazamia, W. T. Huck, J. S. Dennis, A. G. Smith and C. Abell, *Integr. Biol.*, 2011, 3, 1043–1051.
- 17 A. Dewan, J. Kim, R. H. McLean, S. A. Vanapalli and M. N. Karim, *Biotechnol. Bioeng.*, 2012, 109, 2987–2996.
- 18 M. Chen, T. Mertiri, T. Holland and A. S. Basu, *Lab Chip*, 2012, 12, 3870–3874.
- 19 A. Banerjee, R. Sharma, Y. Chisti and U. Banerjee, *Crit. Rev. Biotechnol.*, 2002, 22, 245–279.
- 20 P. Metzger and C. Largeau, *Appl. Microbiol. Biotechnol.*, 2005, 66, 486–496.
- 21 L. Hillen, G. Pollard, L. Wake and N. White, *Biotechnol. Bioeng.*, 1982, 24, 193–205.
- 22 H. Kitazato, S. Asaoka and H. Iwamoto, *J. Jpn. Pet. Inst.*, 1989, 32, 28–34.
- 23 N. L. Jeon, S. K. Dertinger, D. T. Chiu, I. S. Choi, A. D. Stroock and G. M. Whitesides, *Langmuir*, 2000, 16, 8311–8316.
- 24 K. Lee, C. Kim, B. Ahn, R. Panchapakesan, A. R. Full, L. Nordee, J. Y. Kang and K. W. Oh, *Lab Chip*, 2009, 9, 709–717.
- 25 T. Thorsen, S. J. Maerkl and S. R. Quake, *Science*, 2002, 298, 580–584.
- 26 Y. Xia and G. M. Whitesides, *Annu. Rev. Mater. Sci.*, 1998, 28, 153–184.
- 27 A. M. Nonomura, *Jpn. J. Phycol.*, 1988, 36, 285–291.
- 28 M. Grung, P. Metzger and S. Liaen-jensen, *Biochem. Syst. Ecol.*, 1989, 17, 263–269.
- 29 T. L. Weiss, H. J. Chun, S. Okada, S. Vitha, A. Holzenburg, J. Laane and T. P. Devarenne, *J. Biol. Chem.*, 2010, 285, 32458–32466.

- 30 T. L. Weiss, R. Roth, C. Goodson, S. Vitha, I. Black, P. Azadi, J. Rusch, A. Holzenburg, T. P. Devarenne and U. Goodenough, *Eukaryotic Cell*, 2012, **11**, 1424–1440.
- 31 T. Merkel, V. Bondar, K. Nagai, B. Freeman and I. Pinnau, *J. Polym. Sci., Part B: Polym. Phys.*, 2000, **38**, 415–434.
- 32 D. Elsey, D. Jameson, B. Raleigh and M. J. Cooney, *J. Microbiol. Methods*, 2007, **68**, 639–642.
- 33 S. J. Lee, B.-D. Yoon and H.-M. Oh, *Biotechnol. Tech.*, 1998, **12**, 553–556.
- 34 M. W. Toepke and D. J. Beebe, *Lab Chip*, 2006, **6**, 1484–1486.
- 35 S. Okada, T. P. Devarenne, M. Murakami, H. Abe and J. Chappell, *Arch. Biochem. Biophys.*, 2004, **422**, 110–118.
- 36 C. Sorokin and R. W. Krauss, *Plant Physiol.*, 1958, **33**, 109.
- 37 R. Foy, C. Gibson and R. Smith, *Br. Phycol. J.*, 1976, **11**, 151–163.
- 38 S. L. Meseck, J. H. Alix and G. H. Wikfors, *Aquaculture*, 2005, **246**, 393–404.
- 39 Y. Li and J. G. Qin, *J. Appl. Phycol.*, 2005, **17**, 551–556.
- 40 C. Yeesang and B. Cheirsilp, *Bioresour. Technol.*, 2011, **102**, 3034–3040.
- 41 T. Yoshimura, S. Okada and M. Honda, *Bioresour. Technol.*, 2013, **133**, 232–239.
- 42 E. Tyystjärvi and E.-M. Aro, *Proc. Natl. Acad. Sci. U. S. A.*, 1996, **93**, 2213–2218.
- 43 S. Wahal and S. Viamajala, *Appl. Biochem. Biotechnol.*, 2010, **161**, 511–522.
- 44 A. Vonshak, A. Abeliovich, S. Boussiba, S. Arad and A. Richmond, *Biomass*, 1982, **2**, 175–185.
- 45 H. Qiang and A. Richmond, *J. Appl. Phycol.*, 1996, **8**, 139–145.
- 46 S. Watson, E. McCauley and J. A. Downing, *Can. J. Fish. Aquat. Sci.*, 1992, **49**, 2605–2610.
- 47 P. Falkowski and D. A. Kiefer, *J. Plankton Res.*, 1985, **7**, 715–731.

Electronic Supplementary Information

A microfluidic photobioreactor array demonstrating high-throughput screening for microalgal oil production

Hyun Soo Kim¹, Taylor L. Weiss^{2, 4}, Hem R. Thapa², Timothy P. Devarenne^{2*}, and Arum Han^{1, 3*}

¹ Department of Electrical and Computer Engineering, Texas A&M University, College Station, Texas 77843, USA

² Department of Biochemistry and Biophysics, Texas A&M University, College Station, Texas 77843, USA

³ Department of Biomedical Engineering, Texas A&M University, College Station, Texas 77843, USA

⁴ Current address: Department of Biology, Washington University, Saint Louis, Missouri 63130, USA

*Correspondence should be addressed to Arum Han (arum.han@ece.tamu.edu) or Timothy P. Devarenne (tpd8@tamu.edu).

Supplementary Information	Operation principle of a microfluidic binary demultiplexer
Supplementary Fig. S1	Fabrication process of the microfluidic microalgal photobioreactor array
Supplementary Fig. S2	Light interference among neighboring chambers
Supplementary Fig. S3	Experimental setup
Supplementary Fig. S4	Correlation between size and chlorophyll autofluorescence of <i>B. braunii</i> colonies
Supplementary Fig. S5	Microfabricated high-throughput microfluidic microalgal photobioreactor array

Supplementary Fig. S6	<i>B. braunii</i> growth under 16 different light intensities using the developed microfluidic platform
Supplementary Fig. S7	<i>B. braunii</i> growth under 8 different light-dark cycles using the developed microfluidic platform
Supplementary Fig. S8	Different designs of algal colony trapping sites
Supplementary Table S1	Light intensity measured through black-dye-filled light intensity control channel in the microfluidic platform and corresponding light transmittance rate
Supplementary Video S1	Operation principle of the high-throughput microfluidic microalgae cultivation platform

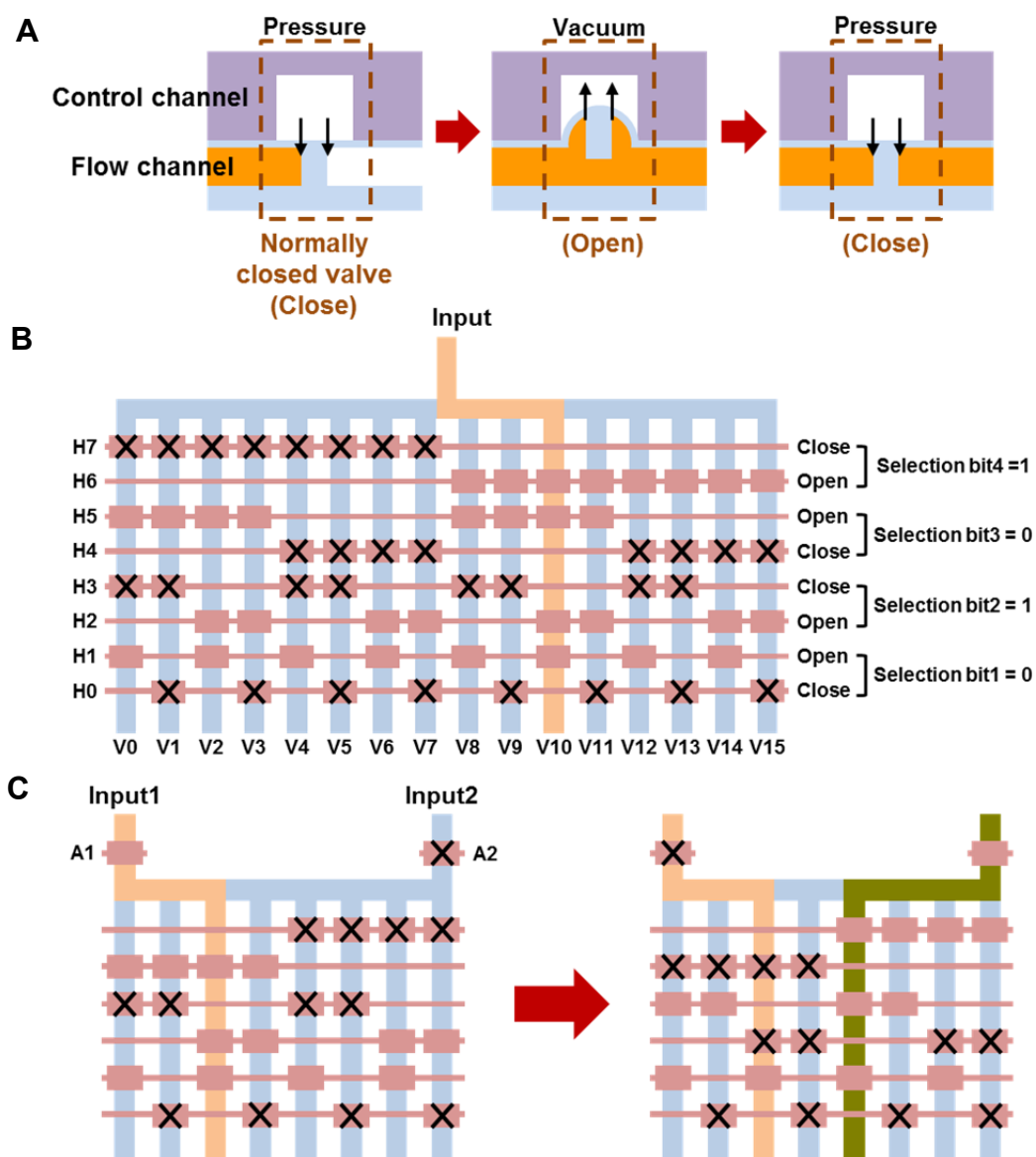
Supplemental Information (SI)

Microfluidic pneumatic binary demultiplexer

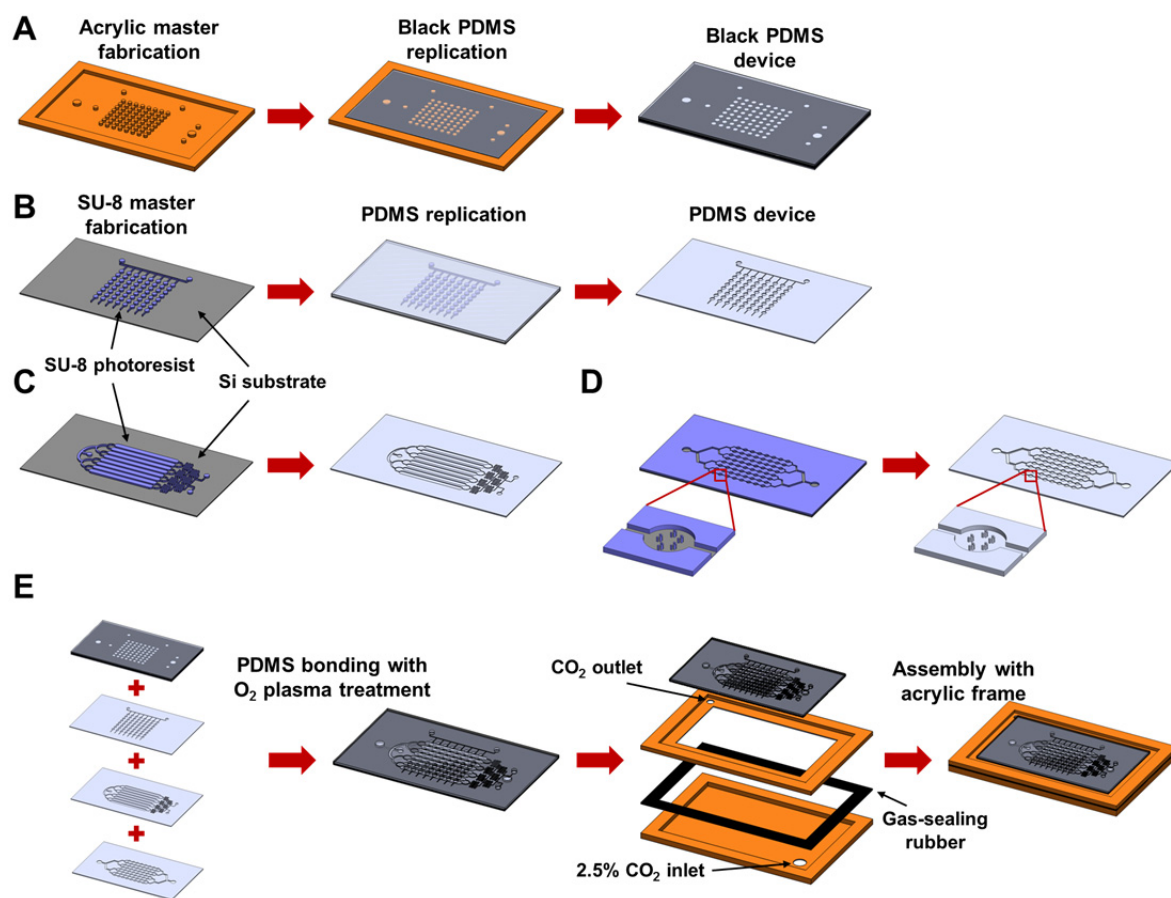
The microfluidic pneumatic binary demultiplexer¹ was composed of two distinct PDMS layers where the control layer containing control lines (H0 – H7 in SI Fig. 1) to actuate microvalve patterns were placed on top of the flow layer comprising of input and output channels to be controlled (V0 – V15 in SI Fig. 1). The microvalve patterns were formed at the junction where the top control lines crossed the bottom flow channels so that the thin membrane between the top and the bottom channels could be deflected by pneumatic actuation. This resulted in opening (negative pressure applied) or closing (positive pressure applied) of the bottom flow channels (SI Fig. 1A).

The pneumatic binary demultiplexer was used to choose one particular channel out of the 16 output channels through which input solution could flow (SI Fig. 1B). Each pair of control channels (4 pairs in total) was connected to a group of microvalves regulating half of the flow channels. Thus, a pair of control channels formed a complementary pair (e.g., H0–H1, H2–H3, H4–H5, and H6–H7), and constituted one selection bit. To open (or select) a single output channel, only one control channel from each complementary valve pair had to be opened (actuated with a negative pressure, “open”) while the other was closed (actuated with a positive pressure, “close”). Thus, the open-close states of the two control channels forming a selection bit were always opposite. For instance, if the selection bit was 0, H0 was closed while H1 was open. On the other hand, if the selection bit was 1, H0 was open and H1 was closed. By deciding the state of each selection bit, opening and closing of the 16 output channels could be independently controlled. For example, when selection bit 1, 2, 3, and 4 were in state 0, 1, 0, and 1, input solution could flow through the selected output channel V10 ($0101_2 = 10$; SI Fig. 1B). Due to the complementary microvalves organized in a binary architecture, 16 output microchannels (N) could be controlled with 8 control microchannels ($2\log_2 N$).

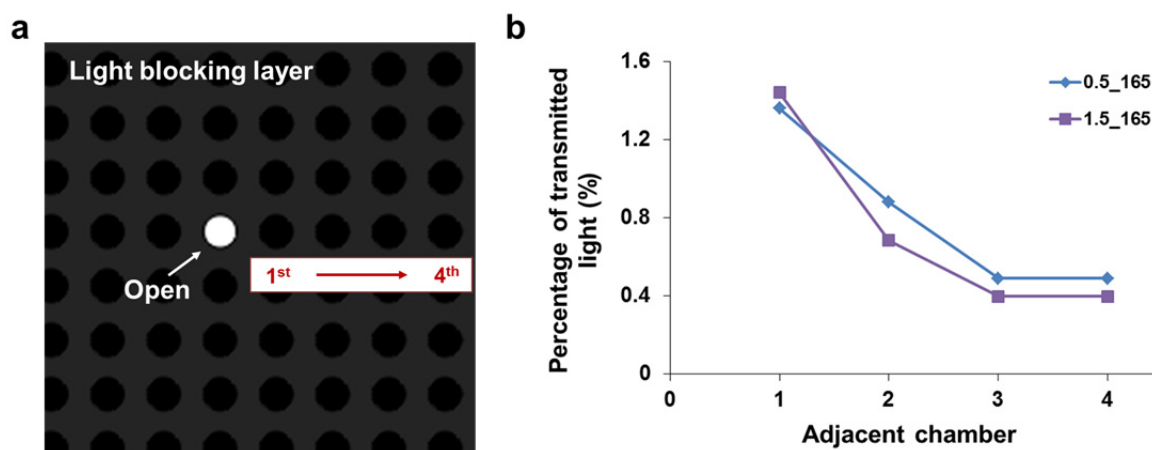
For our developed microalgae photobioreactor array to control the different light-dark cycles, a modified microfluidic pneumatic binary demultiplexer having two inputs (DI water and black dye) instead of a single input as described above was used. The overall working principle in the modified schematic was same, with the only difference being that two additional microvalve structures (A1 and A2 in complementary state) were used to control the two inputs (SI Fig. 1C). Depending on whether A1 was open and A2 was closed, or A1 was closed and A2 was open, either black dye (input 1) or DI water (input 2) could flow into the system. This selected input solution could then flow into one of the 8 output channels selected by the pneumatic binary demultiplexer (SI Fig. 1C).



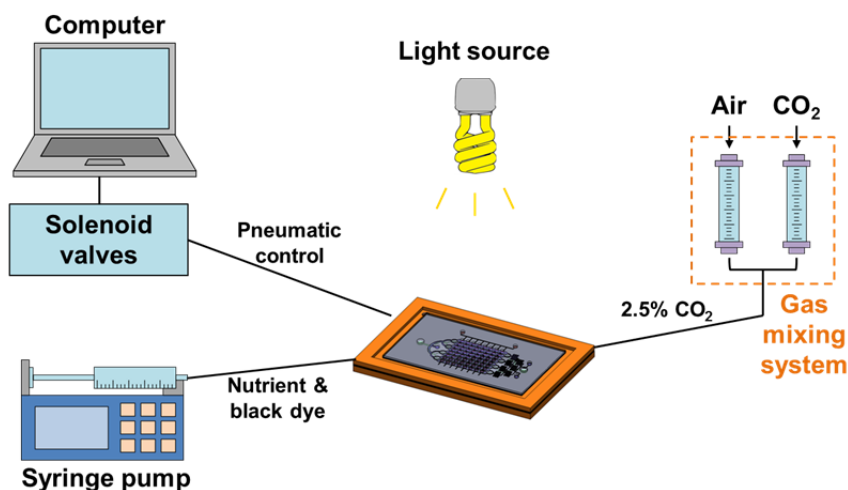
SI Fig. 1. Operation principle of a microfluidic binary demultiplexer. (A) Microvalve composed of a control layer and a flow layer utilized in this demultiplexer. (B) Binary demultiplexer in which 16 output channels were regulated with 8 control microchannels. (C) Modified binary demultiplexer having two inputs and two additional microvalves, which was utilized in the high-throughput microfluidic microalgal photobioreactor array to control different light-dark cycles.



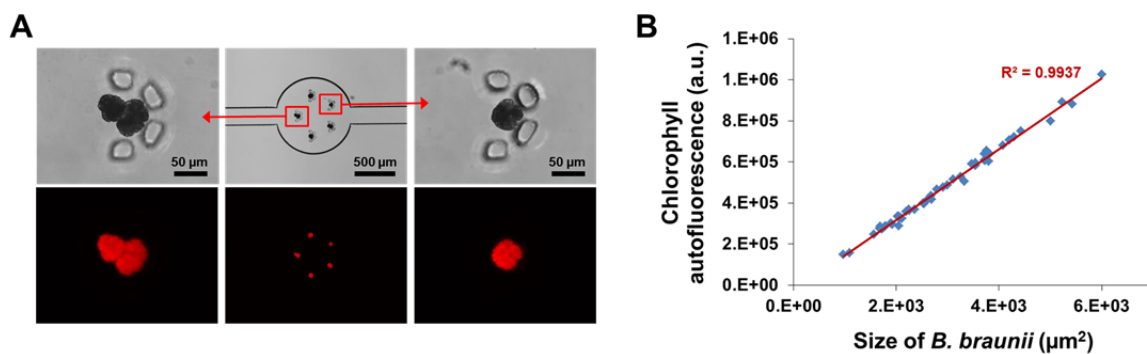
Supplementary Fig. S1. Fabrication process of the microfluidic microalgal photobioreactor array. (A) Light blocking layer. (B) Microfluidic light-dark cycle control layer. (C) Microfluidic light intensity control layer. (D) Microalgae culture layer. (E) Bonding of all PDMS layers using O₂ plasma treatment and assembly into a gas-tight acrylic frame for CO₂-controlled environment.



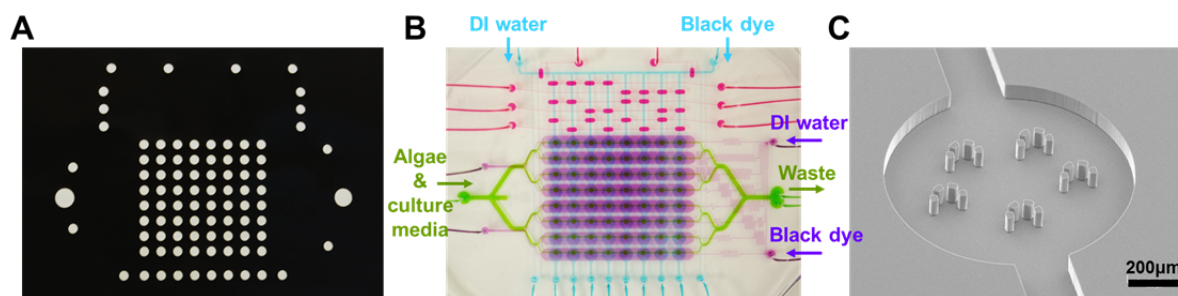
Supplementary Fig. S2. Light interference among neighboring chambers. (A) Schematic showing the setup for this measurement. All chambers in the light blocking layer were blocked except for one chamber (highlighted as “Open”), and the intensities of light underneath this particular chamber as well as adjacent chambers were measured and compared. (B) Comparison of the degree of transmitted light from neighboring chambers by changing the distance from the bottom of the platform used (0.5 and 1.5 in the graph legend indicate 0.5 and 1.5 mm). Number 165 in the graph legend indicates the intensity of incident light, $165 \mu\text{mol photons}\cdot\text{m}^{-2}\cdot\text{s}^{-1}$. Less than 1.5% light transmittance was observed, which is negligible.



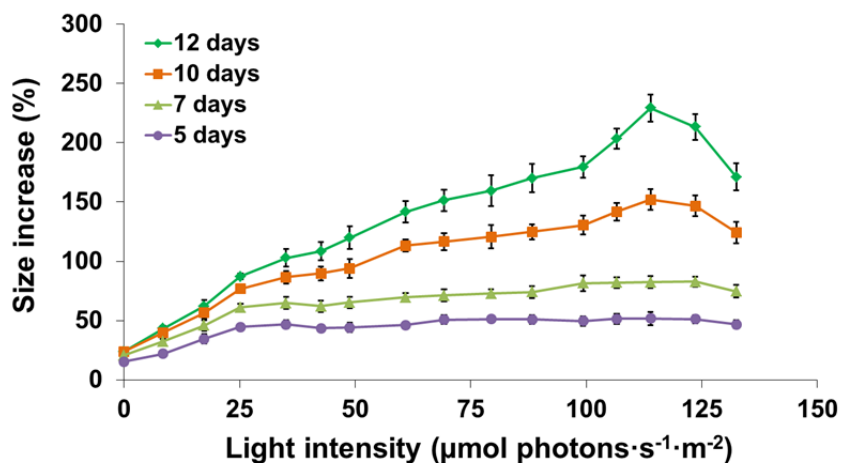
Supplementary Fig. S3. Experimental setup. Air containing 2.5% CO₂ was generated by mixing atmospheric air and 99.9% CO₂ in the ratio of 40 to 1 by controlling each gas flow with compact shielded flowmeters (VWR). This mixed gas was then sterilized through a filter, and flowed into the acrylic culture frame, where CO₂ could diffuse into the microalgae culture compartments through the exposed thin PDMS layer. A 14-W compact fluorescent light bulb (65 K), which could provide different incident intensities of light depending on the distances from the microalgae culture platform, was used. Nutrients were continuously supplied by a syringe pump (1 µl/min, Chemyx Inc.), which introduced fresh culture media into the platform and flushed any waste products out of the platform. The flow of DI water and black dye to produce different light intensities and different light-dark cycles were also controlled with syringe pumps, where different flow rates were used for intensity control (5 µl/min : 0.8 µl/min = DI water : black dye) and light cycle control (1.5 µl/min for both solutions). All control lines in the microfluidic pneumatic binary demultiplexer to regulate the light-dark cycles were operated automatically by an array of solenoid valves and a programmable Labview™ interface.



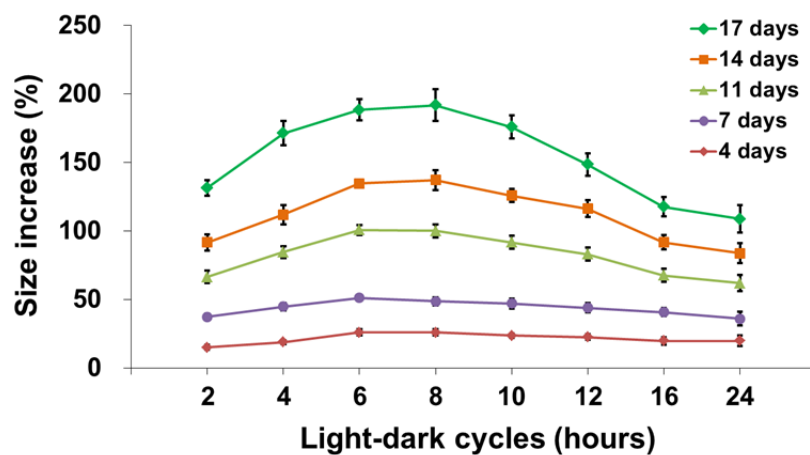
Supplementary Fig. S4. Correlation between size and chlorophyll autofluorescence of *B. braunii* colonies. (A) Chlorophyll autofluorescence and bright field images of captured *B. braunii* colonies inside the platform. (B) Strong linear correlation ($R^2=0.9937$) between *B. braunii* size and intensity sum of its corresponding chlorophyll autofluorescence, which also indicates strong linear relationship between size and biomass.



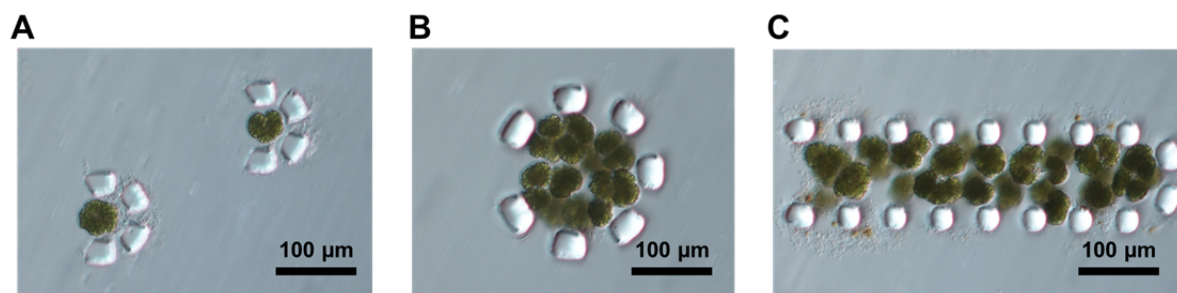
Supplementary Fig. S5. Microfabricated high-throughput microfluidic microalgal photobioreactor array. (A) Light blocking layer. (B) Fully assembled system. Light-dark cycle control layer (cyan: cycle control channels, pink: pneumatic binary demultiplexer) + light intensity control layer (purple) + microalgae culture layer (green) stacked on top of each other. (C) SEM image of a single culture chamber with five *B. braunii* colony trapping sites.



Supplementary Fig. S6. *B. braunii* growth under 16 different light intensities using the developed microfluidic platform. Average size increase of *B. braunii* at days 5, 7, 10, and 12 ($n = 18$) under 16 different light intensities with a 12-hour light-dark cycle were analyzed. Data shown are mean \pm standard error.



Supplementary Figure S7. *B. braunii* growth under 8 different light-dark cycles using the developed microfluidic platform. Average size increase of *B. braunii* at days 4, 7, 11, 14 and 17 ($n = 15$) under 8 different light-dark cycles with a light intensity of $120 \mu\text{mol photons}\cdot\text{m}^{-2}\cdot\text{s}^{-1}$ were analyzed. Data shown are mean \pm standard error.

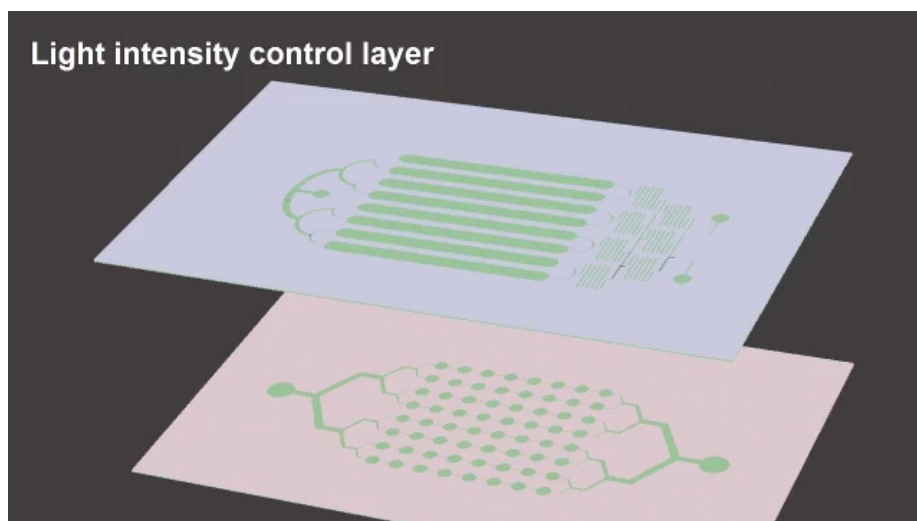


Supplementary Fig. S8. Different designs of algal colony trapping sites. (A) Single-colony trapping design consisting of smaller opening (52 μm). Multiple-colony trapping designs having (B) a large circular structure and (C) a long U-shape structure.

Supplementary Table S1. Light intensity measured through black-dye-filled light intensity control channel in the microfluidic platform and corresponding light transmittance rate.

Light-to-platform distance (cm)	Black dye concentration (%)								
	0 (DI water)	0.3	0.5	1	1.5	2	2.5	3.5	4
	Light intensity ($\mu\text{mol photons}\cdot\text{m}^{-2}\cdot\text{s}^{-1}$)								
4.5	295.40	269.23	252.12	217.31	185.65	163.82	142.05	111.69	97.93
5.6	261.40	238.68	222.86	198.93	172.92	151.98	128.46	103.49	88.76
7.7	175.78	163.50	155.67	132.87	114.87	101.07	85.71	68.44	58.12
9.7	132.44	123.27	114.14	97.68	87.24	77.51	63.35	51.22	44.35
12.7	80.21	73.90	69.54	60.14	52.44	47.25	38.91	30.98	27.01
25	37.01	34.12	33.27	29.06	24.70	21.63	18.03	14.34	12.40
	Transmittance rate (%)								
4.5	100.00	91.14	85.35	73.56	62.85	55.46	48.09	37.81	33.15
5.6	100.00	91.31	85.26	76.10	66.15	58.14	49.14	39.59	33.96
7.7	100.00	93.01	88.56	75.59	65.35	57.50	48.76	38.94	33.06
9.7	100.00	93.08	86.19	73.76	65.87	58.52	47.83	38.67	33.49
12.7	100.00	92.14	86.70	74.98	65.38	58.90	48.52	38.63	33.68
25	100.00	92.20	89.90	78.52	66.75	58.44	48.72	38.75	33.50
Average	100.00	92.15	86.99	75.42	65.39	57.83	48.51	38.73	33.47
Standard deviation	0.00	0.82	1.86	1.82	1.35	1.25	0.48	0.57	0.33

Light-to-platform distance (cm)	Black dye concentration (%)									
	5	6.5	8.5	10	15	20	40	60	80	100
	Light intensity ($\mu\text{mol photons}\cdot\text{m}^{-2}\cdot\text{s}^{-1}$)									
4.5	77.36	52.23	34.96	22.72	7.43	3.98	0.26	0.00	0.00	0.00
5.6	67.54	46.54	28.71	21.46	8.00	3.97	1.04	0.75	0.00	0.00
7.7	45.69	32.48	18.93	13.89	5.58	3.03	1.03	0.54	0.15	0.00
9.7	34.10	23.00	14.30	9.88	4.42	2.12	0.47	0.00	0.00	0.00
12.7	20.51	14.00	9.20	6.70	2.78	1.27	0.28	0.16	0.12	0.00
25	9.42	6.63	4.21	2.84	1.14	0.52	0.09	0.05	0.00	0.00
	Transmittance rate (%)									
4.5	26.19	17.68	11.84	7.69	2.52	1.35	0.09	0.00	0.00	0
5.6	25.84	17.80	10.98	8.21	3.06	1.52	0.40	0.29	0.00	0
7.7	25.99	18.48	10.77	7.90	3.17	1.73	0.58	0.31	0.08	0
9.7	25.75	17.37	10.80	7.46	3.34	1.60	0.36	0.00	0.00	0
12.7	25.57	17.46	11.47	8.36	3.46	1.58	0.35	0.20	0.15	0
25	25.45	17.90	11.38	7.67	3.07	1.41	0.26	0.13	0.00	0
Average	25.80	17.78	11.21	7.88	3.10	1.53	0.34	0.15	0.04	0.00
Standard deviation	0.27	0.40	0.43	0.34	0.33	0.14	0.16	0.13	0.06	0.00



Supplementary Video S1. Operation principle of the high-throughput microfluidic microalgae cultivation platform

Supplementary References

1. T. Thorsen, S. J. Maerkl and S. R. Quake, *Science*, 2002, **298**, 580-584.